Characterizing breast tumor lipid metabolism by integrating magnetic resonance spectroscopic imaging with MALDI mass spectrometric imaging

L. Jiang[1], K. Chughtai[2], D. Artemov[1], P. Winnard Jr.[1], V. Raman[1], Z. Bhujwalla[1], R. Heeren[2], and K. Glunde[1]
[1]ICMIC, Russell H. Morgan Department of Radiology and Radiological Science, Johns Hopkins Medical School, Baltimore, MD, United States, [2]FOM-Institute for Atomic and Molecular Physics, Amsterdam, Netherlands

Introduction: The intensity of the lipid signal in both MR spectroscopic images and mass spectrometric images of tumors is spatially heterogeneous. The heterogeneous physiologic tumor microenvironment may contribute to this heterogeneity. This microenvironment is characterized by abnormal physiologic conditions such as hypoxia and acidic extracellular pH, which is generated largely by the chaotic tumor vasculature and lack of well-established lymphatics. Cancer cells can significantly contribute to this abnormal tumor microenvironment (TME) through increased glycolysis, upregulation of inflammatory pathways, and the secretion of proteolytic enzymes. We therefore investigated the relationship between hypoxia and lipid metabolites in a human breast cancer model by combining *in vivo* magnetic resonance imaging (MRI) and magnetic resonance spectroscopic imaging (MRSI) with *ex vivo* mass spectrometric imaging (MSI) and optical imaging of hypoxia and necrosis.

Methods: Human MDA-MB-231-HRE-tdTomato breast cancer cells, which were genetically engineered to express red fluorescent tdTomato protein under hypoxic conditions, were orthotopically grown in nude mice [1]. Both 3-dimensional (3D) water-unsuppressed MRSI, to detect water, and water-suppressed 3D MRSI to detect metabolites, were performed. Inherently registered 3D T1-weighted images were acquired to measure the tumor anatomic structure as a reference for MRSI. Ponceau S in gelatin based fiducial marker system was developed in order to perform multi-modality image registration and analysis. Each tumor was sectioned to obtain fiducially marked 2-mm thick slices, which were imaged by brightfield and fluorescence microscopy to visualize hypoxic tumor regions. Each 2-mm thick slice was cryo-sectioned into fiducially marked 10-um thick slices to perform MSI, and histologically hematoxylin/eosin (H/E) stained to visualize the necrotic area in the tumor. For MSI, cryo-sections were thaw-mounted on indium tin oxide (ITO)-coated glass slides, and covered with matrix. The matrix consisted of 10mg/mL *alpha*-cyano-4-hydroxycinnamic acid (CHCA) in 50% acetonitrile/0,1% trifluoroacetic acid. Matrix-assisted laser desorption ionization (MALDI) MSI was performed on a modified TRIFT-II instrument as described previously [2, 3] to detect small molecules as well as intact proteins up to 20,000 m/z. To image an entire breast tumor section, the sample stage was moved at 100 µm/s at a laser repetition rate of 10 Hz within a line-scan. Our in-house software Datacube Viewer was used to visualize any mass of interest from the generic data format. We built a co-registration platform based on Ponceau S based fiducial markers and shape characteristics that allowed us to fuse MRI, MRSI, MSI and optical images. The optical hypoxia images were registered to MSI images and H/E stained images based on the fiducial markers. The H/E stained images and the corresponding hypoxic region and necrotic region were registered to the corresponding high-resolution tumor anatomic MRI T1-weighted images along with lipid metabolite images by combining rigid transformation based on the tumor shape characteristics.

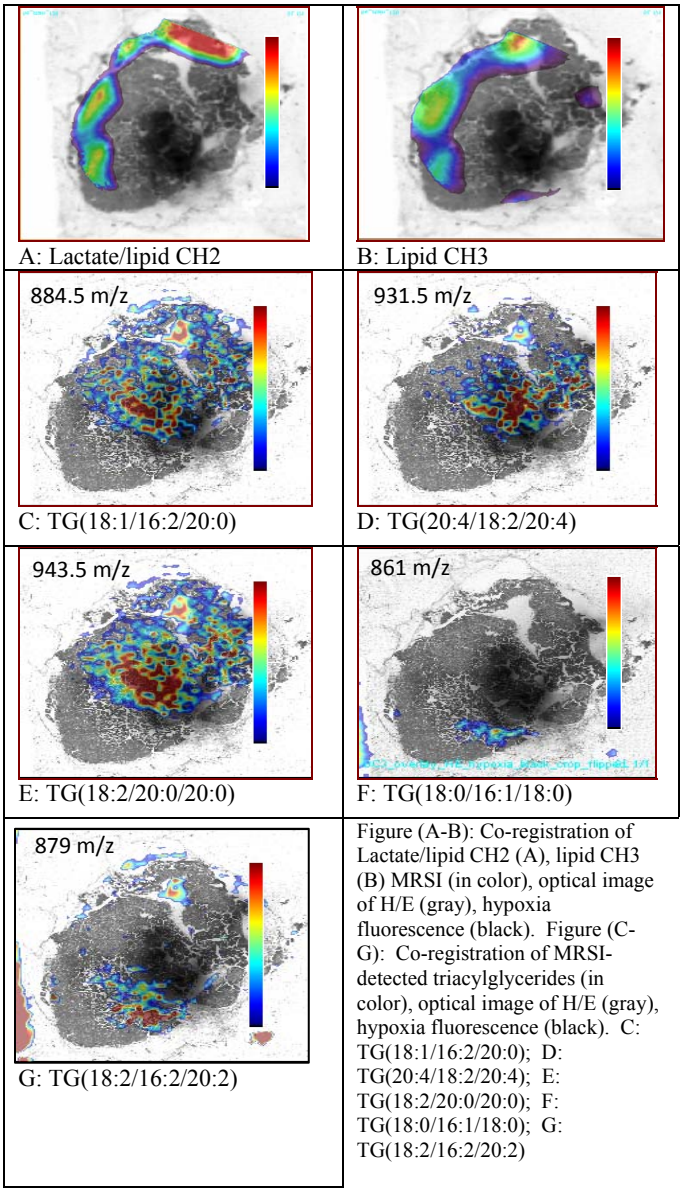

Figure (A-B): Co-registration of Lactate/lipid CH2 (A), lipid CH3 (B) MRSI (in color), optical image of H/E (gray), hypoxia fluorescence (black). Figure (C-G): Co-registration of MRSI-detected triacylglycerides (in color), optical image of H/E (gray), hypoxia fluorescence (black). C: TG(18:1/16:2/20:0); D: TG(20:4/18:2/20:4); E: TG(18:2/20:0/20:0); F: TG(18:0/16:1/18:0); G: TG(18:2/16:2/20:2)

Results: Lactate/lipid CH2 (1.3 ppm), and lipid CH3 (0.9 ppm) were observed in MRSI. Several molecular triacylglyceride (TG) species were observed in MSI. Fig. A and B show the co-registration of hypoxia, H/E stained images, and lipid signals detected by MRSI. Fig C to G show the co-registration of hypoxia, H/E stained images, and lipid signals in MSI of the same breast tissue slice. We observed that lactate/lipid CH2 and lipid CH3 obtained by MRSI were mostly located to the rim region of the tumor slices (Fig A, B) while some TG signals from MSI co-localized with hypoxic regions (Fig C, D, E) and some other TG signals from MSI co-localized with necrotic regions (Fig F, G).

Discussion and Conclusions: MRSI *in vivo* detects CH2 and CH3 groups in fatty acids, which are located mostly in triacylglycerides and other lipids that form mobile lipid droplets [4]. Elevated concentrations of lipid signals detected by MRS were previously demonstrated in necrotic regions [5]. Our ultimate goal in this study is to determine if MRSI detected lipid CH2 and CH3 groups are predominantly localized in hypoxic, necrotic, or normoxic tumor regions, and, with the help of co-registered MSI, identify which molecular TG species contribute to these MRSI-detected lipid signals. Our data revealed that at least three TG species, namely TG(18:1/16:2/20:0), TG(20:4/18:2/20:4), and TG(18:2/20:0/20:0) were partially located to hypoxic regions. At least two TG species (TG(18:0/16:1/18:0), TG(18:2/16:2/20:2)) localized to necrotic regions. In this particular tumor slice, the MRSI-detected lipid signals lactate/lipid CH2 and lipid CH3 localized to viable normoxic tumor regions, and overlapped with TG(18:1/16:2/20:0) and TG(18:2/20:0/20:0). Our fiducially marked co-registration platform allowed us to fuse MRI, MRSI, MSI and optical images in 2D. We are currently extending this platform for application in 3D.

References: [1]. Raman, V., D. Artemov, et al. (2006), *Cancer Res* **66**: 9929-36. [2]. Luxembourg et al. (2004), *Anal Chem* **76**: 5339-44. [3]. Luxembourg et al. (2006), *Rapid Commun Mass Spectrom* **20**: 3435-42. [4]. Calabrese et al. (2008), *Cancer Epidemiol Biomarkers Prev* **17**: 1386-1395. [5]. Opstad, K. S., B. A. Bell, et al. (2008), *NMR Biomed* **21**: 677-85.

Acknowledgements: This work was supported by NIH R01 CA134695. We thank Tiffany Blackwell for technical laboratory support.